



## RUN II DIFFRACTIVE MEASUREMENTS AT CDF

KOJI TERASHI

(For the CDF Collaboration)

The Rockefeller University  
1230 York Avenue, New York, NY 10021, USA  
E-mail: terashi@rockefeller.edu

We present results on hard diffraction obtained by the CDF Collaboration in Run II proton-antiproton collisions at the Fermilab Tevatron. Run I CDF results on hard diffraction are also reviewed.

## 1 Introduction

Diffraction events in  $\bar{p}p$  collisions are characterized by the presence of a leading proton or antiproton which remains intact, and/or a rapidity gap, defined as a pseudorapidity<sup>1</sup> region devoid of particles. Diffractive events involving hard processes (“hard diffraction”), such as production of high  $E_T$  jets (see Fig. 1), have been studied extensively to understand the nature of the exchanged object, the Pomeron, which in QCD is a color singlet entity with vacuum quantum numbers. One of the most interesting questions in hard diffractive processes is whether or not they obey QCD factorization, in other words, whether the Pomeron has a universal, process independent, parton distribution function (PDF). Results on diffractive deep inelastic scattering (DDIS) from the  $ep$  collider HERA show that QCD factorization holds in DDIS. However, single diffractive (SD) rates of  $W$ -boson [1], dijet [2],  $b$ -quark [3] and  $J/\psi$  [4] production relative to non-diffractive ones measured at CDF are  $\mathcal{O}(10)$  lower than expectations from PDFs determined at HERA, indicating a severe breakdown of factorization in hard diffraction between Tevatron and HERA. The suppression factor at the Tevatron relative to HERA is approximately equal in magnitude to that measured in soft diffraction cross sections relative to Regge

---

<sup>1</sup>The pseudorapidity  $\eta$  of a particle is defined as  $\eta \equiv -\ln(\tan \theta/2)$ , where  $\theta$  is the polar angle of the particle with respect to the proton beam direction.

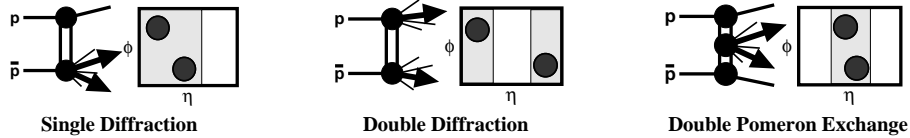


Figure 1: Diagrams and event topologies of dijet production in single diffraction (left), double diffraction (middle) and double pomeron exchange (right).

theory predictions based on Regge factorization. The suppression relative to predictions based on DDIS PDFs is illustrated in Fig. 2, which shows the “diffractive structure function”  $F_{jj}^D$  measured at CDF by using diffractive dijet data with a leading antiproton detected in Roman Pots [5, 6]. The  $\tilde{F}_{jj}^D$  (integrated over antiproton momentum loss  $\xi$  and four momentum transfer squared  $t$ ) was obtained as a function of  $\beta$ , the momentum fraction of the parton in the Pomeron,  $\beta = x_{\bar{p}}/\xi$  ( $x_{\bar{p}}$  is  $x$ -Bjorken of the parton in the antiproton, see Fig. 2), by measuring the ratio of diffractive to non-diffractive dijet rates and using the known leading order PDFs of the proton. The measured suppression of  $F_{jj}^D$  relative to the expectation from the H1 PDFs is approximately equal to that observed in soft diffraction. CDF has also studied dijet events with a double Pomeron exchange (DPE) topology (Fig. 1) using the Roman Pot trigger sample at  $\sqrt{s} = 1800$  GeV [7]. By measuring the ratio of DPE to SD dijet rates ( $R_{SD}^{DPE}$ ) and comparing it with that of SD to ND rates ( $R_{ND}^{SD}$ ), a breakdown of QCD factorization was observed as a discrepancy of the double ratio  $D = R_{ND}^{SD}/R_{SD}^{DPE} = 0.19 \pm 0.07$  from unity.

## 2 Run II Diffraction Measurements

In Run II, being currently under way, CDF plans to study various topics on diffraction, including  $Q^2$  and  $\xi$  dependence of  $F_{jj}^D$  in SD, gap width dependence of  $F_{jj}^D$  in DPE, production of exclusive dijet, heavy flavor and low mass states in DPE, and dijets with a large gap in-between jets. Two recently installed “Miniplug” (MP) calorimeters cover the region  $3.5 < |\eta| < 5.1$ , and 7 stations of scintillation counters, called Beam Shower Counters (BSC), mounted around the beam pipe, extend the coverage to the very forward region of  $5.5 < |\eta| < 7.5$ .

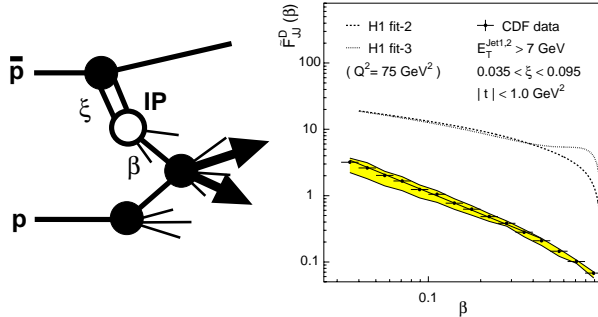


Figure 2: Left: Diagram of diffractive dijet production. Right: Data  $\beta$  distribution (points) compared with expectations from DDIS by H1 (dashed and dotted lines). The straight line is a fit to the data of the form  $\beta^{-n}$ . The filled band represents the range of data expected when different numbers of jets are used in evaluating  $\beta$ . The normalization uncertainty of the data is  $\pm 25\%$ .

The Roman Pots (RP) used in Run I were re-installed and are being operated to trigger on leading antiprotons in the kinematic range  $0.02 < \xi < 0.1$  and  $0 < |t| < 2 \text{ GeV}^2$ .

### 3 Diffractive Dijet Production in Run II

Triggering on a leading antiproton in the RP in conjunction with at least one calorimeter tower with  $E_T > 5 \text{ GeV}$ , a study of diffractive dijet events has been performed. From a sample of 352K triggered events, about 15K SD dijet events with dijets of corrected  $E_T > 5 \text{ GeV}$  in the range  $0.02 < \xi < 0.1$  were obtained. The  $\xi$  (fractional momentum loss of antiproton) was measured by using all calorimeter information. Using a non-diffractive dijet sample triggered on the same calorimeter tower requirement, the ratio of diffractive to non-diffractive dijet rates was measured as a function of  $x$ -Bjorken of the parton in the antiproton, as shown in Fig. 3. This figure shows that (i) the ratio observed with Run II data in approximately the same kinematic region as in Run I reproduces the Run I results, and (ii) there is no appreciable  $\xi$  dependence in the ratio, as already seen in Run I. Measurement of the  $\xi$  dependence at still lower  $\xi$  values ( $\xi < 0.02$ ) is one of our Run II goals and is being currently under study. Preliminary results of the  $Q^2$  dependence of the ratio, where  $Q^2$

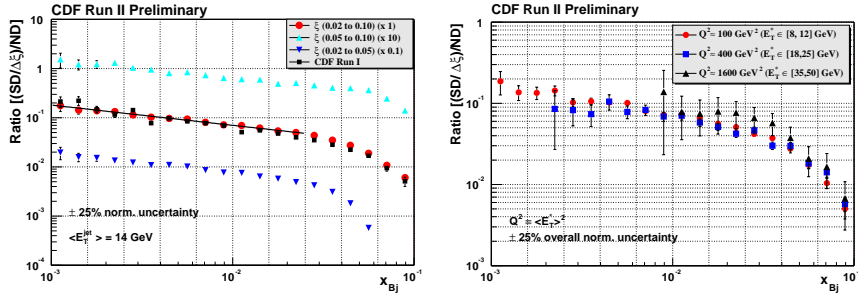


Figure 3: Ratio of diffractive (per unit  $\xi$ ) to non-diffractive dijet rates as a function of  $x$ -Bjorken of the parton in the antiproton. Left: ratios for different  $\xi$  intervals (circle:  $0.02 < \xi < 0.1$ , downward triangle:  $0.02 < \xi < 0.05$ , upward triangle:  $0.05 < \xi < 0.1$ ) for average dijet  $E_T$  of 14 GeV, compared with Run I measurement (square). Right: ratios for different  $E_T^*$  (average jet  $E_T$ ) intervals (circle:  $8 < E_T^* < 12$  GeV, square:  $18 < E_T^* < 25$  GeV, triangle:  $35 < E_T^* < 50$  GeV).  $Q^2$  in this plot is defined as  $Q^2 = \langle E_T^* \rangle^2$ .

is defined as the square of average value of the mean dijet  $E_T$ , are shown in Fig. 3. No significant  $Q^2$  dependence is observed, indicating that the Pomeron evolves with  $Q^2$  in a similar way as the proton.

#### 4 Dijet Production by Double Pomeron Exchange in Run II

For a study of DPE dijets in Run II, a dedicated trigger has been implemented that requires a rapidity gap in the BSC in the outgoing proton direction in addition to the presence of a leading antiproton in the RP and a single calorimeter tower of  $E_T > 5$  GeV. The requirement of a BSC gap on the proton side enhances the DPE signal, as can be seen in the two-dimensional LEGO plot of MP versus BSC hit multiplicity of SD dijet events (Fig. 4). Offline, requiring in addition a gap in the proton-side MP, we obtained about 16K dijet events (about 100 times more data than in Run I), which are qualitatively consistent with DPE dijets. Figure 4 (middle and right) shows the  $E_T$ , mean  $\eta$  and azimuthal angle difference  $\Delta\phi$  of the two leading jets for the DPE candidate events (points). As seen in Run I DPE data, the  $E_T$  distributions look similar to those of SD dijets (histograms), while the mean  $\eta$  and  $\Delta\phi$  show that the

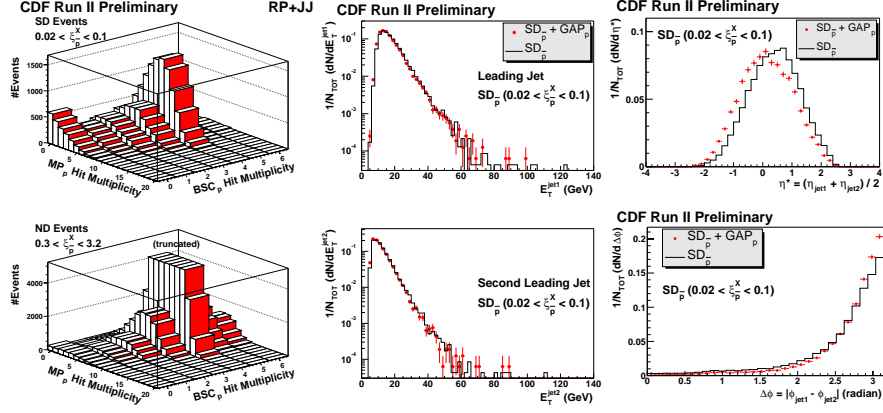


Figure 4: Left: MP hit multiplicity versus BSC hit counter multiplicity on the proton side in SD trigger sample. Events in the region  $0.02 < \xi < 0.1$  ( $0.3 < \xi < 3.2$ ) are shown in the top (bottom) plot. The  $\xi$  is calculated from calorimeter tower information. Middle and Right:  $E_T$  distributions of the leading (middle-top) and second to leading (middle-bottom) jets, mean  $\eta$  (right-top) and  $\Delta\phi$  (right-bottom) of the two leading jets in DPE dijet events (points) compared with those of the SD dijet sample (histograms). All distributions are normalized per unit area.

DPE dijets are more central and more back-to-back.

## References

- [1] F. Abe *et al.*, Phys. Rev. Lett. **78**, 2698 (1997).
- [2] F. Abe *et al.*, Phys. Rev. Lett. **79**, 2636 (1997).
- [3] T. Affolder *et al.*, Phys. Rev. Lett. **84**, 232 (2000).
- [4] T. Affolder *et al.*, Phys. Rev. Lett. **87**, 241802 (2001).
- [5] T. Affolder *et al.*, Phys. Rev. Lett. **84**, 5043 (2000).
- [6] T. Acosta *et al.*, Phys. Rev. Lett. **88**, 151802 (2002).
- [7] T. Affolder *et al.*, Phys. Rev. Lett. **85**, 4215 (2000).